Iraqi Journal of Science

ISSN: 0067-2904

Extinction Cross-Section Modeling of Metallic Nanoparticles

Firas Faeq. K. Hussain[1], Riyadh Mansoor[2], Rasha A. Hussein[2*]
[1]Physics Department, College of Science, Al-Muthanna University, Samawa, Iraq
[2]Engineering College, Al-Muthanna University, Samawa, Iraq

Received: 22/7/2019 Accepted: 21/3/2020

Abstract

Localized surface plasmons (LSPs) are a potentially valuable property for the practical use of small size metallic particles. Exploiting the LSPs in metallic nanoparticle (NP)-based solar cells was shown to increase the efficiency of solar panels. A large extinction cross section of NPs allows for high scattering of light at the surface of the panel, which reduces the panel thickness, allowing for small size and low-cost solar cells. In this paper, the extinction cross-section of spherical nanoparticles is studied and simulated numerically. Surface plasmons were first modeled using the Drude's model then the scattering and absorption cross-sections were derived. Commercial3D simulation software was used to model the near field distribution of the three NP structures. A spherical nanoparticle made of silver was modeled first and the field distribution inside the sphere was presented. The extinction cross-section was also calculated. Two other structures were also presented; a silica NP was first coated with silver shell then a silver NP was coated with silica shell. These structures were studied to estimate the effects of the surroundings on the extinction cross-section. The results show that the silica NP coated with a silver shell provides a high extinction cross-section and can be considered as a good choice for the LSPs-based solar cells.

Keywords: Surface plasmons, metallic nanoparticles, extinction cross-section.

نمذجة المقطع العرضي لقوه الاخماد للجزيئات المعدنية النانوية

فراس فائق[1]، رياض منصور[2]، رشا حسين[2*]
[1]قسم الفيزياء، كلية العلوم، جامعة المثنى ، السماوه، العراق
[2]كلية الهندسة ، جامعة المثنى، السماوه، العراق

الخلاصة

تُعد خاصية البلازمونات السطحية LSPs ذات اهميه كبيره للاستخدام العملي في الجزيئات المعدنية النانويه. أن استغلال خاصيه LSPs في الخلايا الشمسية القائمة على الجسيمات النانوية المعدنية (NP) يزيد من كفاءة الألواح الشمسية. يسمح المقطع العرضي الكبير للانقراض في الجسيمات النانويه NPs بتشتت الضوء بدرجة كبيرة على سطح اللوحة ، مما يقلل من سماكة اللوحة و يسمح بتصنيع خلايا شمسية صغيرة الحجم ومنخفضة التكلفة.

في هذه البحث ، تمت دراسة المقطع العرضي للانقراض (قوه الاخماد) للجسيمات النانوية الكروية من خلال المحاكاه العدديه. درست البلازمونات السطحية أولاً باستخدام نموذج Drude ثم تم اشتقاق المقاطع العرضية للتشتت والامتصاص. تم استخدام برنامج محاكاة ثلاثي الابعاد لنمذجة توزيع المجال القريب من ثلاثة هياكل.

*Email: rasha.lasereng@mu.edu.iq

تم في البدايه دراسه جسيمات نانوية كروية مصنوعة من الفضة حيث تمت دراسه توزيع المجال الكهرومغناطيسي داخل الكرة وكذلك تم حساب المقطع العرضي للانقراض. كما تم االقتراح هيكلين آخرين (يتم طلاء الجسيمات النانوية السيليكا بقشرة فضية أولاً ثم الفضة المطلية بقشرة السيليكا). تتم دراسة هذه الهياكل لتقدير تأثير المناطق المحيطة على المقطع العرضي للانقراض. أظهرت النتائج أن السيليكا المطلي بقشرة فضية يوفر مقطعًا كبيرًا للانقراض ويمكن اعتباره اختيارًا جيدًا للخلايا الشمسية المعتمدة على LSPs.

Introduction

Solar cells are a solution to the increased demand for environmentally friendly energy sources [1]. Solar cells are devices that use the photovoltaic effect to convert sunlight photon energy into electricity. Photovoltaic power has the potential to meet the growing needs of the expanding population since the amount of radiation striking the earth's surface is 1.76 × 105 terawatts (TW) and the current world usage is estimated above 15 TW [2]. However, the cost of photovoltaic modules is still high compared to other renewable energy sources. Reducing the per Watt cost is a principle driving force behind the proposing of the second generation of thin film solar cells (SCs). Thin film SCs technology focuses on reducing the thickness to the range of 1 - 2 µm as well as improving the energy conversion [3]. However, reducing the thickness affects the trapping of light inside the SC, resulting in low light absorption and reduced conversion efficiency. A new generation of SC is being researched with the aim of improving the efficiency of thin film SCs by exploiting the plasmonic effect [4].

The plasmonic effect exists mainly in metals where electrons are weakly bound to the atom and free to move. Surface plasmon polaritons (SPPs) are bound electromagnetic excitations existing at the dielectric-metal interface; resonance coupling between SPPs and light results in enhanced near-field waves. It is either localized or exists as a propagating surface plasmon [5]. The existence of localized surface plasmons (LSPs) is an outstanding optical property of small size metallic particles. For plasmonic SCs, the LSP is exploited to improve the scattering and hence increasing the light trapping of the desired frequency [6].

Optical properties induced in metallic nanoparticles are hardly achievable without the excitation of surface plasmon. A wide range of applications could become achievable by exploiting these properties through an engineered design of NP. Surface plasmon resonance occurs when an electromagnetic field at light frequencies illuminates nanoparticles. A collection of conduction electrons is excited, which leads to their oscillation. If the size of the particle is in the nano-regime and comparable to the wavelength of light illuminating it, this oscillation will result in the excitation of a surface plasmon and the nanoparticle behaviour is highly modified compared to that of macroscopic bulk particles. Overcoming the diffraction limit of traditional optics as well as increasing the sensitivity of optical sensors are some of the possibilities provided by surface plasmon that are encouraging the investigation of other possibilities such as amplification, concentration, and manipulation of light at the nanoscale to introduce a wide range of applications. Bio-medical sensors, information technology, environment protection, and solar cells are examples of these applications [7, 8] . Nanoparticles are solid particles with sizes ranging from a few nanometres to several hundreds of nanometres, having properties that differ significantly from those of bulk materials. Metal NPs have unique optical properties that arise from the large density and susceptibility of their free electrons. EM field results in the displacement of conducting electrons from the positive metal lattice. However, the attraction force will act as a restoring force to return the cloud of electrons to its original levels. A resonance behaviour will lead to the excitation of LSP. The shape and size of the particle is of great importance to determine the resonant frequency of the LSPP modes. The frequency band for spherical NPs is in the visible band while that of cylindrical NPs is near red shifted. In addition, the quality factor of modes for gold nanorods is higher than that of spherical counterpart due to the lower ohmic loss in the near red band compared to the visible region. Near-field optical techniques are used for studying particle plasmon interactions and field enhancement at sub-wavelength scales. However, as soon as the inter-particle distance is large compared to the optical wave- length, far-field optical methods can address individual particles in an experimentally less demanding way, while still providing valuable information.

Excitation of LSPs inside the NPs originates from the electron oscillations that are excited by light. Therefore, a partial extinction of light energy will occur due to the excitation of the LSPs. The

scattering cross-section of a particle is a measure of the absorption efficiency for the incident light. The absorption cross section corresponds to the geometrical section and mainly depends on the radius of the NPs. In addition to the absorption, NPs also cause a scattering for the incident light. Therefore, another quantity must be considered to study the interaction between light and NPS, that is, the scattering cross section. The sum of scattering and absorption cross-sections is the extinction cross-section which is of interest in this work. For very small particles, absorption is more important than scattering, while scattering becomes more important than absorption when the radius of the particle is comparable to the wavelength of light. In this paper, the field distribution along a spherical NP is modelled to simulate the excitation of the LSP. The extinction cross-section is compared for three NP structures. NP made of silica coated with silver is shown to provide higher extinction cross-section compared with that of silver NP and silver coated with silicon. Higher extinction cross- section reduces the absorption length, allowing for high absorption efficiency in thin film solar cells.

The remaining of this paper is organized as follows: section 2 introduces the fundamentals of surface plasmons while the theoretical modelling of the SP is presented in section 3. Numerical modelling of the three structures is presented in section 4. Finally, the conclusions are derived in section 5.

Extinction cross-section in metallic nanoparticles

If the interface between two materials, one with free charge carriers and negative permittivity (such as metal) and the other with positive permittivity, is illuminated with electro- magnetic energy at light frequencies, the resulting quantized oscillations are called surface plasmons. Excitation of the surface plasmon is not restricted only to nanoparticles. Films, wires, and nanorods also exhibit this behaviour. However, the confinement of electrons in leads to localized compared to the extended propagated along the metal-dielectric interface in wires and films. S corresponds to the interaction between light and matter. Therefore, to analyse SP, Maxwell's equations with appropriate boundary conditions need to be solved. When a nanoparticle is illuminated, the light energy forces almost all the freely moving electrons inside the NP to move towards the surface. Thus, accumulation of positive charge in one side and negative charge in another side would occur. This is similar to an electric dipole. However, the dipole effect generates another force to return electrons to equilibrium. Returning electrons to the equilibrium position, in fact, occurs when the nanoparticle oscillates at a specific frequency.

Based on the principle of the conservation of energy, the amplitude of electron oscillation can be obtained indirectly from the amount of light depletion. Increasing the amplitude of electron oscillation requires an increase of energy (kinetic and electrostatic) which should be provided by light. The larger oscillation means high extinction of light inside the NP and a larger excitation of the surface plasmon. As a result, the optical absorption and scattering spectra are good indicators for SP excitation in metallic nanoparticles.

Absorption and scattering cross-sections of a particle are indications of the absorption and scattering efficiencies, respectively. Thus, the SP excitation efficiency is obtained by calculating both absorption and scattering cross-sections and the sum of these two cross sections is called the extinction cross-section. The extinction ratio represents the efficiency of the nanoparticle in extracting the photon energy from the incident beam to the bonded electrons and generating SP. For eNP in the range of 100 nm, the extinction cross section can reach the particle size. However, for small NP (few nanometers), a large extinction cross section (about 10 times the geometrical section) can be achieved.

Metallic nanoparticles that support localized surface plasmon can enhance the light path length inside solar cells and increase the absorption of light. The LSP is mainly affected by the size, shape and the dielectric properties of the surrounding media.

In order to describe the response of a metallic nanoparticle illuminated by the electro- magnetic field of light, the Drude's model needs to be used [9]. The motion equation of the free electrons based on the Drude's model starts from

$$m_e \frac{\partial^2 r}{\partial t^2} + m_e \gamma_d \frac{\partial r}{\partial t} = eE_0 e^{-i\omega t} \quad (1)$$

where r is the displacement of the electron from the centre, $\underline{\gamma}_d$ describes the damping term, m_e is the effective free electron mass, e is the free electron charge, ω and Eo are the frequency and amplitude of the applied electric field, respectively.

The displacement is:

$$r(\omega) = \frac{e}{m_e}\frac{E}{\omega^2 + j\omega\gamma_d} \quad (2)$$

The polarizability (P) is

$$P = \frac{-Ne^2}{m_e}\frac{E}{\omega^2 + j\omega\gamma_d} \quad (3)$$

The dielectric displacement (D) and the dielectric constant (ε) are:

$$D = \varepsilon_o E + P = \varepsilon_o \varepsilon_r = \varepsilon_o\left(1 - \frac{{\omega_p}^2}{\omega^2 + j\gamma\omega}\right) \quad (4)$$

$$\tilde{\varepsilon_r}(\omega) = 1 - \frac{{\omega_p}^2}{\omega^2 + j\gamma\omega} \quad (5)$$

$$\tilde{\varepsilon_r}(\omega) = 1 + \chi(\omega) \quad (6)$$

$${\omega_p}^2 = \frac{Ne^2}{m_e\varepsilon_o} \quad (7)$$

where $\chi(\omega)$ is the susceptibility of the material. Equation (4) gives the plasmon frequency and N is the number of atoms per unit volume of the material.

Beer's law [10] describes the exponential decay of the intensity of a light beam in a medium as:

$$I(x) = I_o \exp(-\alpha x) \quad (8)$$

The absorption constant can then be determined as:

$$\alpha(\omega) = 2k(\omega)/\omega$$

where k(ω) is the extinction coefficient calculated from the complex refractive index [10]

$$\check{n} = n + jk = \mp\sqrt{\tilde{\varepsilon_r}(\omega)} \quad (9)$$

where n and k are the refractive index and the extinction index, respectively.

Plasmon resonance of spherical NPs

Consider a metallic sphere of radius and complex dielectric constant which is illuminated by a light wave of an electric field in a surrounding medium with dielectric constant. The electric field can be calculated by finding the solution of the Poisson equation for the electrical potential [11].

$$E = -\nabla\emptyset(r,\theta)$$

where ∇ is the del operator.

But

$$\nabla.D = 0$$
$$\nabla.(\varepsilon E) = 0$$
$$\nabla.(\varepsilon(-\nabla\emptyset) = 0$$

This results in

$$\nabla.\nabla\emptyset = 0$$

which is the Laplace equation.

$$\nabla^2\emptyset = 0$$

In order to obtain the electric field, the Laplace equation $\nabla^2\emptyset = 0$ should be solved first.

In spherical coordinates, the Laplace equation is given in equation (5):

$$\frac{1}{r^2}\frac{\partial}{\partial r}\left(r^2\frac{\partial\emptyset}{\partial r}\right) + \frac{1}{r^2}\frac{1}{sin\theta}\frac{\partial}{\partial\theta}\left(sin\theta\frac{\partial\emptyset}{\partial\theta}\right) + \frac{1}{r^2 sin\theta^2}\frac{\partial^2\emptyset}{\partial\emptyset^2} = 0 \quad (10)$$

The general solutions for the potential inside ($\emptyset_s$) and outside ($\emptyset_d$) the metallic sphere are given as below:

$$\emptyset_s(r,\theta) = \sum_{l=0}^{\infty} A_l r^l P_l(cos\theta) \tag{11}$$

$$\emptyset_d(r,\theta) = \sum_{l=0}^{\infty} (B_l r^l + C_l r^{-l-1}) P_l(cos\theta) \tag{12}$$

where A, B and C are constants which will be determined by applying boundary conditions, $\emptyset_d = \emptyset_{scatter} + \emptyset_o$ is the potential outside the sphere, which consists of the incoming and scattered parts of the potential.

At the interface r $= a$, the boundary conditions for the tangential part of the electrical field are

$$\partial_\theta \emptyset_s = constant$$

where s is applied for the sphere and for the surrounding medium. Also, the displacement field (the longitudinal part) is

$$\varepsilon_i \partial_r \emptyset_s = constant$$

By applying the above boundary conditions, the potentials inside and outside the sphere can be evaluated as in equations (8) and (9):

$$\emptyset_s(r,\theta) = -\frac{3\varepsilon_d}{\varepsilon_s + 2\varepsilon_d} E_o r cos\theta \tag{13}$$

$$\emptyset_d(r,\theta) = -E_o r cos\theta + \frac{\varepsilon_s - \varepsilon_d}{\varepsilon_s + 2\varepsilon_d} E_o \frac{a^3}{r^2} cos\theta \tag{14}$$

Recall that $\emptyset_d = \emptyset_o + \emptyset_{scatter}$
Therefore,

$$\emptyset_{scatter} = \frac{\varepsilon_s - \varepsilon_d}{\varepsilon_s + 2\varepsilon_d} E_o \frac{a^3}{r^2} cos\theta$$

By multiplying the top and bottom by r, we have

$$\emptyset_{scatter} = \frac{\varepsilon_s - \varepsilon_d}{\varepsilon_s + 2\varepsilon_d} \frac{a^3}{r^3} E_o r cos\theta \tag{15}$$

The electric field can then be expressed as

$$E_s = \frac{3\varepsilon_d}{\varepsilon_s + 2\varepsilon_d} E_o \tag{16}$$

and

$$E_d = E_0 + \frac{\varepsilon_s - \varepsilon_d}{\varepsilon_s + 2\varepsilon_d} \frac{a^3}{r^3} E_o \tag{17}$$

The external field induces a dipole moment P inside the sphere, which is defined as

$$P = 4\pi\varepsilon_o \varepsilon_d a^3 \frac{\varepsilon_s - \varepsilon_d}{\varepsilon_s + 2\varepsilon_d} E_o \tag{18}$$

However, the polarizability can be obtained from the relation $P = \varepsilon_o \varepsilon_d \rho E_o$. Then,

$$\rho = 4\pi a^3 \frac{\varepsilon_s - \varepsilon_d}{\varepsilon_s + 2\varepsilon_d} \tag{19}$$

To obtain the scattering cross section of a metal sphere NP, the ratio of the total radiated power of the dipole to the intensity of the exciting wave should be calculated.
The scattering cross section is

$$\sigma_{scatter} = \frac{8\pi}{3} k^4 a^6 \left| \frac{\varepsilon_s - \varepsilon_d}{\varepsilon_s + 2\varepsilon_d} \right|^2 \quad (20)$$

where k is the magnitude of the wave vector of the incident light.
Using Poynting's theorem [12], the absorption cross-section is as in 15.

$$\sigma_{abs} = 4\pi k a^3 Im(\frac{\varepsilon_s - \varepsilon_d}{\varepsilon_s + 2\varepsilon_d}) \quad (21)$$

Finally, the extinction cross section is defined as the sum of the absorption and scattering cross-sections, as below

$$\sigma_{ext} = \sigma_{abs} + \sigma_{sca} \quad (22)$$

Results

CST Simulations

In this section, a commercial electromagnetic simulation software package is used to calculate the extinction cross-section numerically. CST Studio Suite was used, which is a 3D simulation package that uses the Finite Element Method (FEM) to solve Maxwell's equation in the frequency domain. Three spherical NPs are modelled in this work, as shown in Figure-1. The aim of these calculations is to optimize the NP structure in order to obtain the highest extinction cross-section, which leads to improved characteristics for solar cells. A silver nanoparticle was modelled first, then it was compared with a silica sphere coated by silver shell and another sphere made of silver coated by silica shell, as shown in Figure-1. The optical properties of the layered plasmonic shell [13] were studied and presented. These calculations show the effects of material used along with the effects of changing the surroundings.

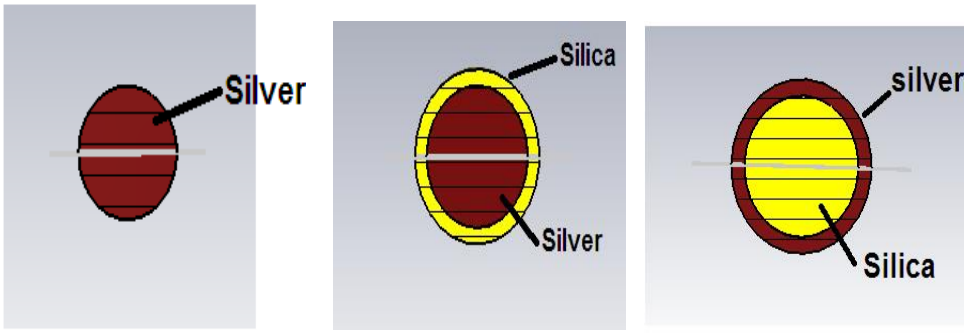

Figure 1-The three structures used in simulations. Left is silver NP, middle is a silver coated with silica and right is a silica coated with silver.

Silver NP

A spherical nanoparticle was modelled first with silver material surrounded by air. The radius of the sphere was 50 nm, and the frequency range was 350 to 1100 THz. Open boundaries were applied in all direction with two symmetry planes. The electromagnetic field was modelled by applying a plane wave, as shown in Figure 2, and a field monitor to estimate the distribution of the electric field along the axis of the sphere was defined. Figure 3 shows how the field is concentrated on the outer surface of the sphere due to the displacement of free electron excited by the electric field. Excitation of surface plasmons is shown in Figure 4. This plasmon is called a bright plasmon due to the scattering of light [14].

Another important quantity that needs to be calculated is the extinction cross-section, which is used to estimate the effects of the nanoparticles in absorption and scattering of the plane wave. Based on the law of conservation of energy, the energy photons will be absorbed by free electrons causing coherent oscillations that excite the surface plasmons. Figure 5 shows the absorption and scattering sections of the silver NP. In this figure, the absorption cross-section is lower than the scattering due to the relatively large size of the NPs. A 62000 nm2 extinction cross section was obtained, as shown in Figure-6.

Figure 6 shows a major peak of about 64000 nm2 at approximately 765 THz with FWHM = 100 THz, which corresponds to the high amount of scattering at this frequency. The graph also shows a localized peak at 870 THz, which is caused by the high absorption shown in Figure-5.

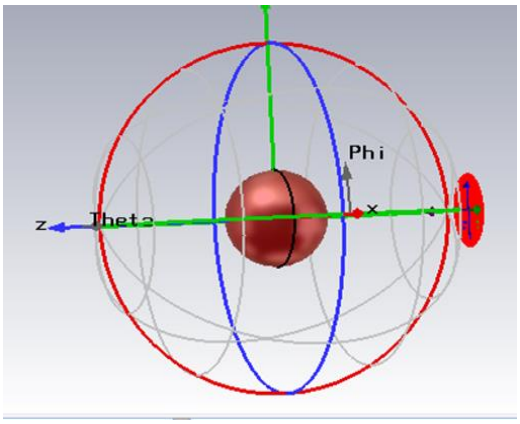

Figure 2-The plane wave representation.

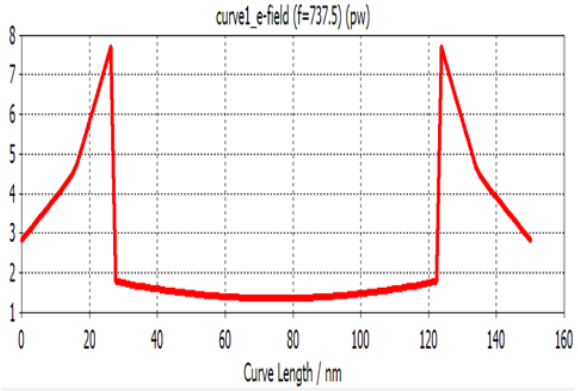

Figure 3-Normalized electric field distribution along the sphere. X axis represents the curve line along the sphere. There is almost no field distribution along the sphere from 20 nm to 120nm with two peaks in each side of the sphere due to the boundary conditions.

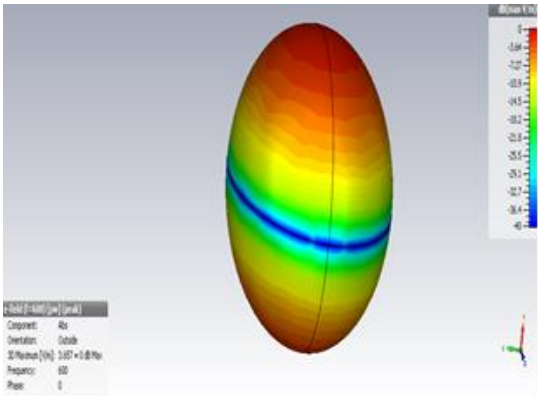

Figure 4-3D filed distribution on the sphere surface

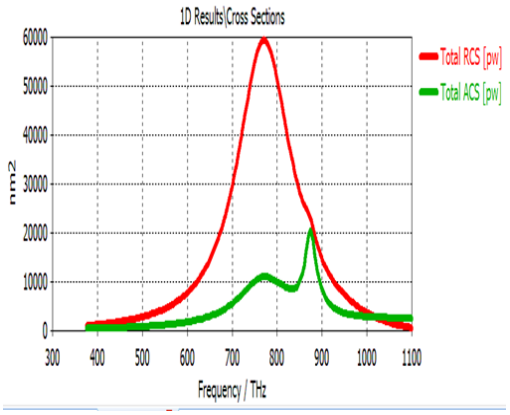

Figure 5-Scattering (green line) and absorption (red line) cross-sections of silver NP.

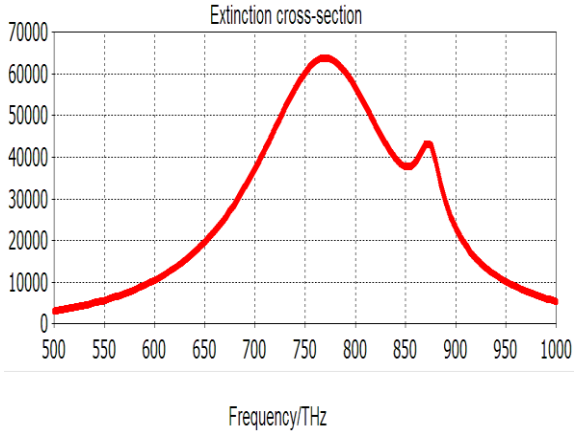

Figure 6-The extinction cross-section. Y axis is in nm units.

Silver coated with silica

A dielectric shell is added to the silver sphere to model the effects of the surroundings on the extinction ratio. The radius of the structure is kept the same as in structure 1. This was achieved by modelling a silver sphere with a radius of 40 nm and a silica shell of 10 nm thickness [15]. Similar steps were performed, and the results are presented in the figures below. The field distribution across the sphere is shown in Figure 7; a comparison between this figure and Figure 2 shows the effects of the two boundary regions, one between the silver and silica dielectric and the other between the dielectric and free space. Figure 8 shows the absorption and scattering cross-sections of this structure. In this structure, no substantial change in the extinction cross-section was obtained, as shown in Figure 9.

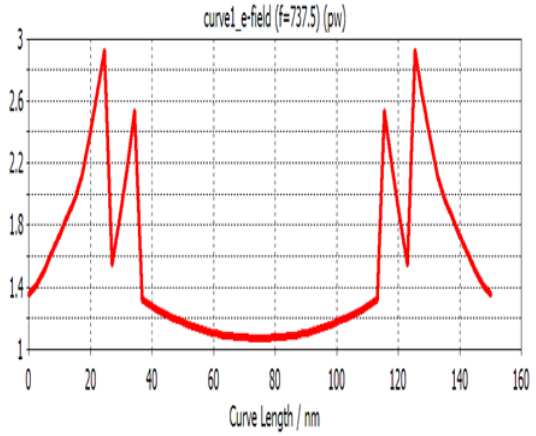

Figure 7- Normalized electric field distribution along the sphere. Two peaks are shown at the silver/silica interface and the silica/air interface.

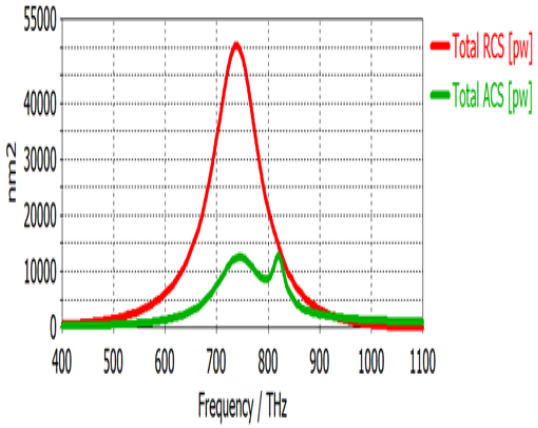

Figure 8- Scattering (green line) and absorption (red line) cross-sections of silver coated with silica.

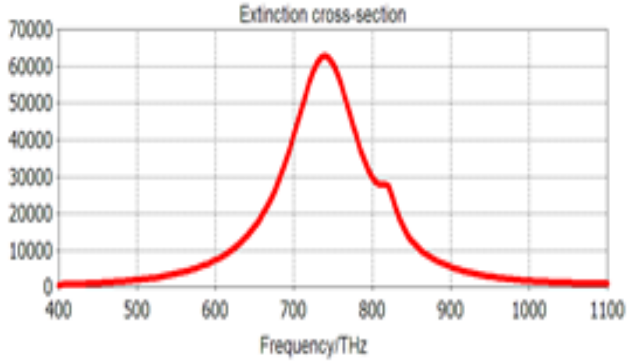

Figure 9- The extinction cross-section. FWHM =120 THz.

Silica-coated with silver shell

Here, a sphere made of silica was modelled first then a shell of silver was used as coating. A 40 nm radius sphere made of silica was modelled first, then a silver shell of 10 nm thickness was applied. Figure 10 shows the field distribution across the sphere; it can be seen that there is a field inside the silica sphere compared to that in Figures-(3 and 7), then the field goes to zero at the interface between the silica and silver shell. The effect of the localized surface plasmon is shown at the outer surface where the field distribution is high.

The scattering and absorption cross sections are shown in Figure 11. This figure shows high scattering cross-section compared to that of the absorption due to the presence of silver shell. This is also noticed in Figure 5 for the silver sphere, while in Figure 8 the silica shell improved the absorption cross-section. Figure 12 shows the high extinction cross-section obtained in this structure compared to the previous structures. A high extinction cross-section is obtained within a small range of frequencies

(fullwidth at half maximum FWHM = 63 THz) which provides a high Q factor compared with the other structures. A summary of the extinction cross section for each structure is presented in Table-1.

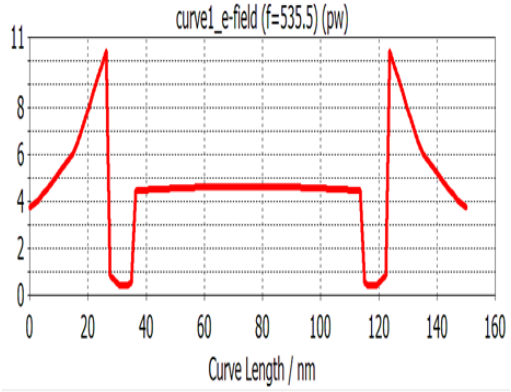

Figure 10- Normalized electric field distribution along the sphere. There is a field distribution inside the sphere due to the electron distribution of the dielectric material. This field goes to zero at the silver shell before it rises at the silver air interface.

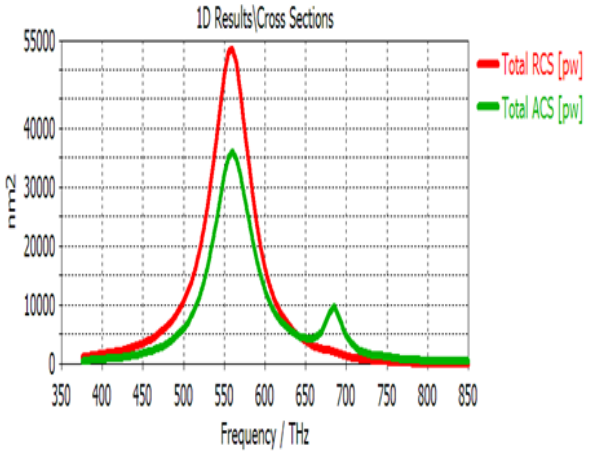

Figure 11-Scattering and absorption cross-section of silica-coated with silver shell.

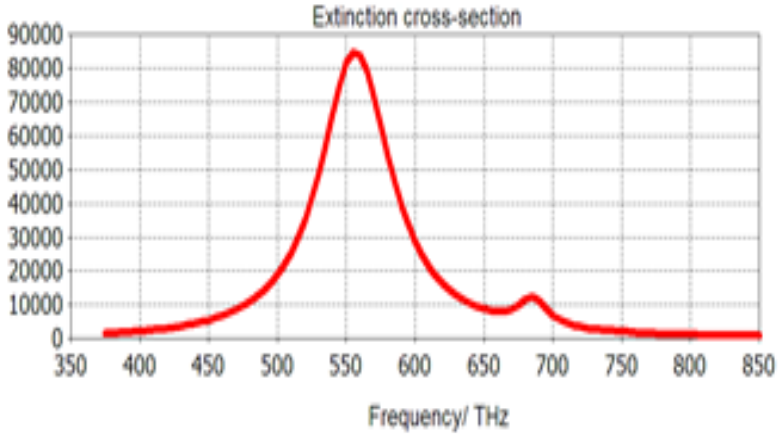

Figure 12- The extinction cross-section of silica-coated with silver shell.

Table 1- Scattering, absorption and extinction cross-section comparison for the three structures

	Scattering cross-section nm^2	Absorption cross-section nm^2	Extinction cross-section nm^2
Silver	55800	8000	63800
Silver coated with silicon	51100	12600	63700
Silica coated with silver	53400	32000	85000

Conclusions

Localized surface plasmons were studied and simulated numerically. The optical response of a spherical nanoparticle is presented in this paper. Surface plasmons are of great interest in many fields of technology, ranging from solar cells to optical biosensing. In this work, theoretical and numerical modelling of the LSPs in silver-based nanoparticles were presented. Absorption and scattering cross-sections of spherical nanoparticles illuminated by a plane wave are calculated. A comparison between three structures of the sphere in terms of the extinction ratio is presented. The silver NPs were modelled first then compared with two structures; in the first one the silver NPs were coated with a silica shell while in the second one the silver NPs were used as a coating for silica NPs. It was shown

that, for the silver NPs, the scattering cross-section was maximum. However, it was reduced with the use of silica shell and reached to minimum with the silicon NPs. However, the extinction cross-section was maximum for silicon NPs coated with silver. The field distribution along the NPs is also presented to show the excitation of the LSPs. Improving the extinction cross-section is of great importance in the fabrication of small size, low cost, solar cells by increasing the absorption of light in small thickness layers.

References

1. Saga, T. **2010.** Advances in crystalline silicon solar cell technology for industrial mass production. *Npg Asia Materials*, **2**(3): 96-102.
2. Atwater, H. A. and Polman, A. **2010.** Plasmonics for improved photovoltaic devices. *Nature Materials*, **9**(3): 205-213.
3. Liu, M., Johnston, M. B. and Snaith, H. J. **2013.** Efficient planar heterojunction perovskite solar cells by vapour deposition. *Nature*, **501**(7467): 395-398.
4. Green, M. A. and Pillai, S. **2012.** Harnessing plasmonics for solar cells. *Nature Photonics*, **6**(3): 130-132.
5. Mansoor, R. and AL-Khursan, A. H. **2018.** Numerical modelling of surface plasmonic polaritons. *Results in Physics*, **9**: 1297-1300.
6. Pillai S. *et al*, **2007.** Surface plasmon enhanced silicon solar cells. *J. of App. Physics,* **101**(109)*:* 093105.
7. Huang C., *et al*, **2012.** Gold nanoring as a sensitive plasmonic biosensor for on-chip DNA detection. *App. Phys. Letter* **100**(17): 173114.
8. Mansoor, Riyadh D. and Alistair Duffy. **2019** "Enhancement of the Surface Plasmon Polaritons Excitation Efficiency." Journal of Southwest Jiaotong University 54.5.
9. Liu, N., *et al*, **2009.** Plasmonic analogue of electromagnetically induced transparency at the Drude damping limit. *Nature Materials*, **8**(9): 758-762.
10. Hodgkinson, J., Masiyano D. and Tatam, R. P. **2009.** Using integrating spheres as absorption cells: path-length distribution and application of Beer's law. *Appl. Opt*. **48**(30): 5748-5758.
11. Hackbusch, W. **2005.** The Poisson Equation. *Elliptic Differential Equations*, 27-37.
12. Alù A. and Engheta, N. **2005.** Achieving transparency with plasmonic and metamaterial coatings. *Physical Review E*. **72**(1): 016623.
13. Alu A. and Engheta, N. **2008.** Multifrequency optical invisibility cloak with layered plasmonic shells. *Phys. Rev. Lett*. **100**(11): 113901.
14. Su X., *et al*, **2010.** Plasmonic interferences and optical modulations in dark-bright-dark plasmon resonators. *Appl. Phys. Lett*. **96**(4): 043113.
15. Oubre C. and Nordlander, P. **2004.** Optical properties of metallodielectric nanostructures calculated using the finite difference time domain method. *J. of Phys. Chemist. B*, **108**(46):17740-17747.